Theoretical study of Pr^{3+}:ZBLAN upconversion ultraviolet fiber laser based on $4f5d$ state

Aiping Fang (方爱平)[1], Zhenwen Dai (戴振文)[1,2], Tao Luo (罗 涛)[1], Guijuan Sun (孙桂娟)[1], Lijun Wang (王立军)[2], and Zhankui Jiang (蒋占魁)[1]

[1] *College of Physics, Jilin University; Key Lab of Coherent Light, Atomic and Molecular Spectroscopy, Ministry of Education, Changchun 130023*

[2] *Key Lab of Excited State Physics, Changchun Institute of Optics, Fine Mechanics and Physics, Chinese Academy of Sciences, Changchun 130021*

Received August 20, 2004

A theoretical study of the kinetics of two-step-excitation upconversion ultraviolet cw fiber laser based on the $4f5d$ state in Pr^{3+}:ZBLAN is performed using steady population rate equations and light propagation equations. Under different Pr^{3+} concentrations, the dependence of the threshold pump powers on the other pump power, the variations of laser output power with reflectivity of output coupler, pump powers and fiber length as well as the dependence of the optimum fiber length on pump powers are investigated. The results predict some optimum laser parameters for maximizing output power.

OCIS codes: 140.3510, 140.3610, 160.5690, 190.7220.

Tunable ultraviolet (UV) lasers have many important applications in physics, chemistry, biology, and other fields. Most of known tunable UV laser sources are excimer lasers or complicated devices comprising some tunable lasers in visible or infrared region and subsequent nonlinear frequency conversion. These systems are complicated and bulky, and such drawbacks greatly restrict their applications. Therefore, it is much necessary and of great interest to study the simple, reliable, cheap and high-efficiency tunable UV laser sources, which are in favor of small all-solid-state tunable UV lasers.

The $4f^{N-1}5d$ energy levels of trivalent rare-earth (RE) ions doped in hosts have quite broad UV absorption and emission spectra[1]. Obviously, the $4f^{N-1}5d$ levels are possible and perfect upper laser levels for broad-band tunable UV laser. Tunable UV lasers based on $5d$ upper levels have been realized in Ce^{3+}:$LiCaAlF_6$/$LiLuF_4$ crystals pumped by direct 4ω or 5ω excitation of Nd^{3+}:YAG laser[2]. Since $4f^{N-1}5d$ direct excitation occurs in or near the vacuum UV region, the pumping source itself is a complex UV laser bringing an additional complexity to the system. A significant approach for this problem is the frequency upconversion excitation of $4f^{N-1}5d$ levels using the upconversion pump mechanisms. Upconversion visible lasers in some RE-doped crystals and fibers have been realized based on $4f^N$ intraconfigurational transitions[3]. Among the various RE ions doped in hosts, Pr^{3+} has a lower 5d energy distribution except for Ce^{3+} ion[4]. Ce^{3+} has only two adjacent $4f$ levels and hence its $5d$ levels cannot be excited by effective upconversion pump. Pr^{3+} is a preferred dopant for investigating upconversion UV laser based on $5d$ upper levels. Recently, the $4f5d$ upconversion excitation in Pr^{3+}:$LiYF_4$/$LiLuF_4$ was reported[5].

In fluoride glasses, the fluorozirconate ZBLAN (ZrF_4-BaF_2-LaF_3-AlF_3-NaF) glass has been proved to be a rather good sort of optical and laser material[6]. This glass is of high transmission from infrared to UV region (230—8000 nm) and it can be fabricated into optical fiber. Moreover, because the highest phonon energy in ZBLAN is not more than 600 cm^{-1}[7], much higher upconversion pump efficiency can be obtained in such glass than in oxide glasses[8]. As a laser medium, the advantages of fiber include high pump intensity in core, good heat-removal and easily structuring small all-solid-state laser.

To our knowledge, studies on the $5d$ upconversion UV laser have not been reported by now. To realize this kind of laser in practice, a theoretical study of its performance is necessary. In this letter, utilizing the theory of steady population rate equations and light propagation equations, we investigate the $5d$ upconversion UV laser kinetics in Pr^{3+}:ZBLAN fiber based on the laser transition from $4f5d$ to the ground state $^3H_4$.

Figure 1 shows an energy level diagram for Pr^{3+} in ZBLAN together with level labels, pumping scheme and laser transition. Two-step resonant pump was used for $4f5d$ upconversion excitation. The first pump laser (λ_1= 478 nm) excites Pr^{3+} from the lowest Stark level of $^3H_4$ to $^3P_0$ and the second one (λ_2= 329 nm) excites Pr^{3+} from $^3P_0$ to one of the $4f5d$ levels by excited-state absorption. By advance calculations for the upconversion excitation kinetics, we found that population inversion can occur between $4f5d$ and the higher Stark level of $^3H_4$. In this letter, the highest Stark level of $^3H_4$ is chosen as the lower laser level of $4f5d$ upconversion UV laser and the laser wavelength λ_s is 197 nm.

The composition of ZBLAN fiber studied is $52ZrF_4$-$20BaF_2$-$4LaF_3$-$4AlF_3$-20NaF. To study the concentration effect on laser process, five Pr^{3+} concentrations 1000, 2000, 3000, 4000 and 5000 ppm in weight were considered. Here we consider a fiber Fabry-Perot laser having two cavity mirrors M_1 and M_2 with signal reflectivities R_1 and R_2. We assume that $R_1 = 99\%$ and $R_2 = 1 - 2\% - T$ where 2% is the signal loss on M_2 and T is the transmission factor of M_2. A top-hat function assuming that light intensities are constant inside the fiber core and zero outside is used for the transversal power distributions in the fiber[9].

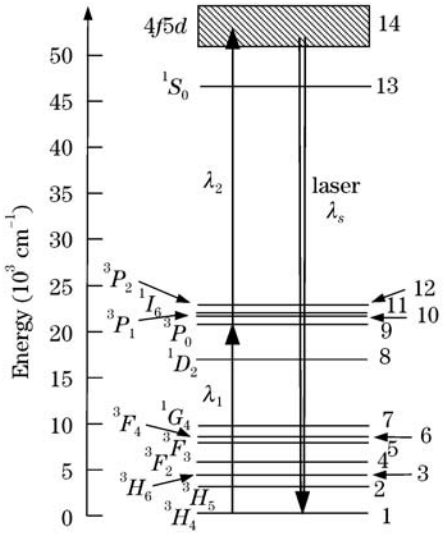

Fig. 1. Energy level diagram of Pr^{3+} ions in Pr^{3+}:ZBLAN.

Rate equations for the population density of each level shown in Fig. 1 are expressed as

$$\frac{\mathrm{d}n_j}{\mathrm{d}t} = \sum_{i=j+1}^{14} A_{ij}n_i - \sum_{i=1}^{j-1} A_{ji}n_j, j \neq 1, 9, 14, \quad (1)$$

$$\frac{\mathrm{d}n_9}{\mathrm{d}t} = R_{19}n_{1L} - R_{91}n_9 - R_{9\ 14}n_9 + R_{14\ 9}n_{14} + \sum_{i=10}^{14} A_{i9}n_i - \sum_{i=1}^{8} A_{9i}n_9, \quad (2)$$

$$\frac{\mathrm{d}n_{14}}{\mathrm{d}t} = R_{9\ 14}n_9 - R_{14\ 9}n_{14} + W_{1\ 14}n_{1H} - W_{14\ 1}n_{14} - \sum_{i=1}^{13} A_{14\ i}n_{14}, \quad (3)$$

$$\sum_{i=1}^{14} n_i = 1, \quad (4)$$

where n_i is the normalized population density (NPD) of the ith level, n_{1L} and n_{1H} are NPDs of the lowest and highest Stark level of the ground state $^3H_4$, respectively. A_{ij} is the spontaneous transition rate, while R_{ij} and W_{ij} are the pump and the signal stimulated transition rates, respectively.

A_{ij} includes radiative rate A_{ij}^{rad} and nonradiative rate W_{ij}^{non}. A_{ij}^{rad} comprises three main terms: the electric dipole A_{ij}^{ed}, the magnetic dipole A_{ij}^{md}, and the quadrupole A_{ij}^{eq}. For a transition within $4f^2$ configuration, A_{ij}^{ed} can be calculated by the Judd-Ofelt theory[10,11].

The intensity parameter Ω_λ depends on Pr^{3+} concentration[12], the reduced matrix element takes the data in Pr^{3+}:LaF_3[13]. The transition wavenumber σ are from Refs. [14,15]. A_{ij}^{md} and A_{ij}^{eq} can be calculated by the magnetic-dipole and higher-order-electric transition theories[16]. The radial integral $\langle 4f\,|r^2|\,4f\rangle$ needed for A_{ij}^{eq} calculation is taken as 1.464 a.u.[17]. In general, because the two terms are much smaller than the A_{ij}^{ed} term, the influence of dopant concentration on them is neglectable. Since the electric dipole transition between $4f^2$ and $4f5d$ levels is parity-allowable, only the A_{ij}^{ed} term is important to A_{ij} and given by

$$A_{ij}^{\mathrm{ed}} = \frac{64\pi^4\sigma^3}{3h\Gamma}\frac{n\left(n^2+2\right)^2}{9}e^2\left|\langle 4f\,|r|\,5d\rangle\right|^2, \quad (5)$$

where Γ is the statistical weight of one $4f5d$ level, and $\langle 4f\,|r|\,5d\rangle = 0.9$ a.u.[17].

W_{ij}^{non} can be calculated by[18]

$$W_{ij}^{\mathrm{non}} = W_0\mathrm{e}^{-\alpha\Delta E}, \quad (6)$$

where W_0 and α are nonradiation parameters, ΔE is the energy gap. W_0 and α take 1×10^8 s^{-1} and 0.005 cm respectively, which are the typical values for LaF_3[18].

The relations between R_{ij}, W_{ij}, A_{ij} and the cross section σ_{ij} are

$$R_{ij} = \frac{P_k(z)\,\sigma_{ij}}{\pi a^2 h\nu_k}, \quad k = 1, 2, \quad (7)$$

$$W_{ij} = \frac{P_{\mathrm{tot}}(z)\,\sigma_{ij}}{\pi a^2 h\nu_s}, \quad (8)$$

$$\sigma_{ij} = \frac{A_{ij}\lambda^2}{8\pi n^2\Delta\nu}, \quad (9)$$

where a is the fiber core radius assumed as 0.5 μm, $P_{1,2}$ are the pump powers of λ_1 and λ_2, the spectral bandwidth $\Delta\nu$ is taken as 10^{10} Hz corresponding to a typical linewidth of narrow lines in RE doped hosts. P_{tot} is the total guided power of signal laser and under neglect of amplified spontaneous emission it is written as $P_{\mathrm{tot}} = P_s^+ + P_s^-$, where P_s^+ and P_s^- are the forward and backward signal powers, respectively.

Assuming the pump waves make single transit from one end of the fiber ($z = 0$) in the forward direction (+), the propagation equations of them are given by

$$\frac{\mathrm{d}P_1}{\mathrm{d}z} = -\left(n_{1L}\sigma_{19} - n_9\sigma_{91}\right)n_tP_1 - \beta_1P_1, \quad (10)$$

$$\frac{\mathrm{d}P_2}{\mathrm{d}z} = -\left(n_9\sigma_{9\ 14} - n_{14}\sigma_{14\ 9}\right)n_tP_2 - \beta_2P_2, \quad (11)$$

where n_t is the total population density of Pr^{3+} and $\beta_{1,2}$ are background losses of $P_{1,2}$. The bi-directional propagation equations for the signal wave are stated as

$$\frac{\mathrm{d}P_s^\pm}{\mathrm{d}z} = \pm\left(n_{14}\sigma_{14\ 1} - n_{1h}\sigma_{1\ 14}\right)n_tP_s^\pm \mp \beta_sP_s^\pm, \quad (12)$$

where β_s is the background loss of the signal. The boundary conditions of Eq. (12) are

$$P_s^+(z=0) = R_1P_s^-(z=0), \quad (13)$$

$$P_s^-(z=L) = R_2P_s^+(z=L), \quad (14)$$

where L is the fiber cavity length.

Using the transition parameters introduced above and the steady rate Eqs. (1)—(4) together with propagation Eqs. (10)—(12), threshold pump power, output power, and optimum cavity length were obtained.

Threshold pump power can be calculated by using the threshold condition[19] $2\bar{g}_0L = \delta$, where $\bar{g}_0$ is the averaged small signal gain in the cavity, $\delta = 2\beta_sL - \ln(1-T)$ is

the total signal loss. Note that the gain coefficient g of the fiber medium is a function of the launched pump powers $P_{1,2}$ and the fiber coordinate z. Therefore g has the form

$$g\left(P_{1,2},z\right)=\left[n_{14}\left(P_{1,2},z\right)\sigma_{14\ 1}-n_{1H}\left(P_{1,2},z\right)\sigma_{1\ 14}\right]n_t. \tag{15}$$

In calculations, by taking an average of length we can obtain the averaged small signal gains $\bar{g}_0\left(P_{1,2}\right)$ only relevant to $P_{1,2}$. The pump powers when $\bar{g}_0\left(P_{1,2}\right)=\bar{g}_0$ correspond to the threshold pump powers. Figure 2 shows λ_1 threshold pump power versus launched λ_2 pump power for various Pr^{3+} concentrations when $R_2=70\%$, $L=12$ m and $\beta_{1,2,s}=0.1$ dB/m. Once λ_2 power is larger than a certain value (for example, 75 mW for 5000 ppm), the minimum of λ_1 threshold power is obtained and remains constant with the change of λ_2 power. By comparison, if λ_2 power is less than that value, λ_1 threshold power has a dramatic increase and tends to infinity as λ_2 power decreases. Therefore, it can be thought that the actual threshold pump power appears at the turning point of each curve in Fig. 2. λ_2 threshold power has similar dependences on λ_1 power as shown in Fig. 3. It can be obviously seen that the coordinates of the two turning points for a Pr^{3+} concentration in Figs. 2 and 3 are the same. Also it is seen that the minimum of threshold power is related to the Pr^{3+} concentration. Owing to threshold power of λ_1 larger than that of λ_2, λ_1 power should be

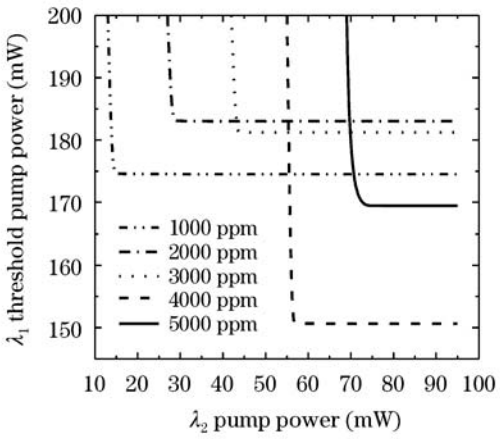

Fig. 2. λ_1 threshold pump power versus λ_2 pump power.

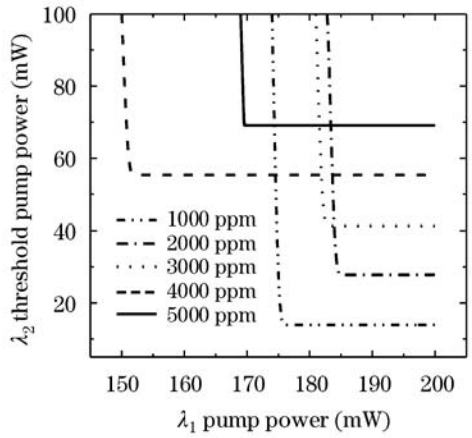

Fig. 3. λ_2 threshold pump power versus λ_1 pump power.

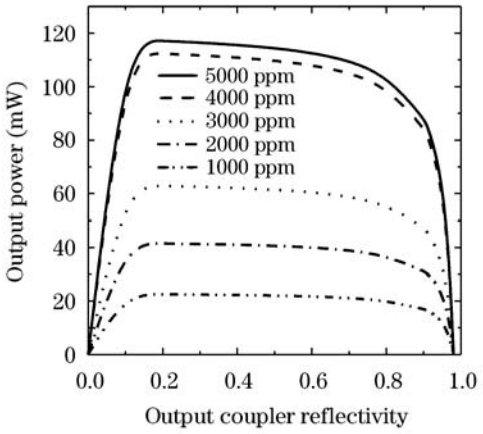

Fig. 4. Output power versus output coupler reflectivity.

suitably higher than λ_2 power so as to make full use of pump energy λ_1 power. But for simplicity, we assume that λ_1 and λ_2 powers are equal in below calculations.

The plots of laser output power versus R_2 for various Pr^{3+} concentrations at 400 mW pump powers and for different pump power at 5000 ppm are shown in Figs. 4 and 5, respectively. All the curves in the two figures have similar shapes and cut the horizontal axis in two places: one is the low-reflectivity intersections near zero and the other is the high-reflectivity intersections at $R_2=98\%$ due to the 2% loss of M_2. Output power changes dramatically at smaller or larger R_2 while it changes little and has a higher value as R_2 goes from 20% to 70%. Therefore, R_2 was taken as 70% in below calculations.

A plot of output power versus pump powers for several L values under 5000 ppm is shown in Fig. 6. It is seen that the threshold and the slope efficiency are related to L. When L is small, pump energy cannot be well absorbed and hence threshold and slope efficiency are lower. Both threshold and slope efficiency increase with L and tend to fixed values. At 5000 ppm concentration, the maximum of slope efficiency is up to 10%.

Output power as a function of L for several pump powers under 5000 ppm is shown in Fig. 7, in which all the curves intersect the horizontal axis at the positions near zero because fiber cavity of short L cannot provide enough stimulated radiation to sustain laser oscillation. Each curve has a peak corresponding to the maximum

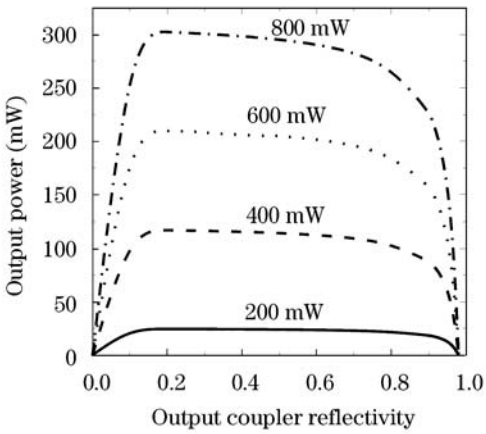

Fig. 5. Output power versus output coupler reflectivity.

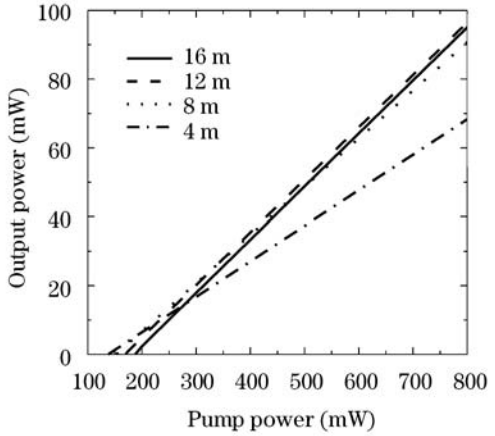

Fig. 6. Output power versus launched pump powers.

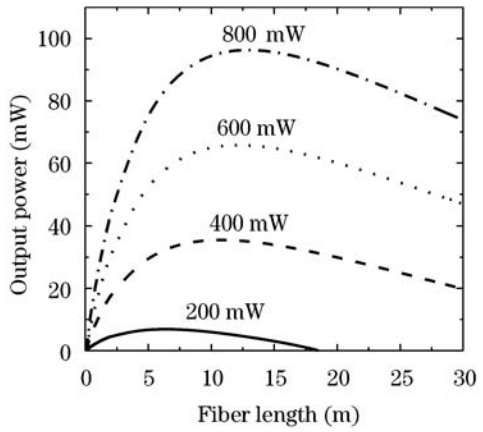

Fig. 7. Output power versus the fiber length.

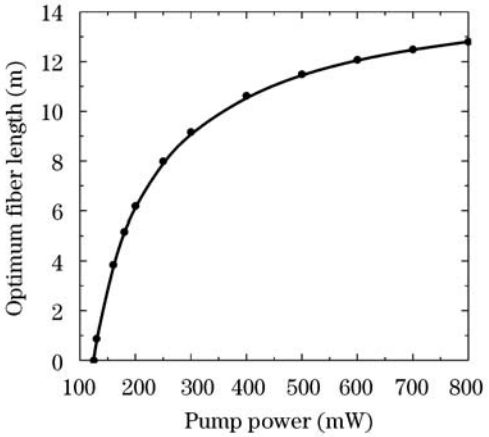

Fig. 8. Optimum fiber length versus pump powers.

output power. The fiber length of this case can be called the optimum fiber length (L_0). When $L = L_0$, one of the pump lights is just all absorbed at the end of fiber. When $L > L_0$, output power almost linearly decreases because population inversion exists over only $0 \leq z \leq L_0$ and in the region of $z > L_0$ there is background loss but no stimulated emission. Therefore, given the laser characteristics (such as R_1, R_2, P_1, P_2 and β_s), an optimum fiber length is required to get maximum output power. Figure 7 also shows that higher pump powers need a larger L_0 to produce a higher optimum output power.

The optimum fiber length is defined as the fiber length for the maximum output power when other laser characteristics are fixed. The optimum fiber length depends on the laser characteristics especially the pump powers. Figure 8 is a graph of optimum fiber length versus pump powers. Under smaller pump powers, the optimum fiber length increases quickly with pump powers. When pump powers large enough, it becomes a constant.

In summary, using the rate equations and propagation equations, we investigated the potentiality to produce upconversion UV cw laser based on two-step $4f5d$ excitation in Pr^{3+}:ZBLAN fiber. The results predict the dependence of threshold pump powers, output power and fiber optimum cavity length on the other characteristic parameters of the laser. For a 12 m fiber, slope efficiency of the laser can achieve 10%.

This work was supported by the National Science Foundation of China (No. 10104009). Z. Dai is the author to whom the correspondence should be addressed, his e-mail address is dai@jlu.edu.cn.

References

1. W. S. Heaps, L. R. Elias, and W. M. Yen, Phys. Rev. B **13,** 94 (1976).
2. Z. L. Liu, H. Ohtake, N. Sarukura, M. A. Dubinskii, V. V. Semashko, A. K. Naumov, S. L. Korableva, and R. Y. Abdulsabirov, Japan J. Appl. Phys. **36,** L1384 (1997).
3. E. Osiac, E. Heumann, G. Hubert, S. Kuck, E. Sani, A. Toncelli, and M. Tonelli, Appl. Phys. Lett. **82,** 3832 (2003).
4. P. Dorenbos, J. Lumin. **87—89,** 970 (2000).
5. S. Nicolas, E. Descroix, M. F. Joubert, Y. Guyotet, M. Laroche, R. Moncorge, R. Y. Abdulsabirov, A. K. Naumov, V. V. Semashko, A. M. Tkachuk, and M. Malinowski, Opt. Materials **22,** 139 (2003).
6. D. C. Hanna, Phil. Trans. Roy. Soc. Lond. A **354,** 779 (1996).
7. R. M. Almeida and J. Mackenzie, J. Chem. Phys. **74,** 5954 (1981).
8. R. S. Quimby, M. G. Drexhage, and M. J. Suscavage, Electron. Lett. **23,** 32 (1987).
9. A. C. Tropper, J. N. Carter, R. D. T. Lauder, D. C. Hanna, S. T. Davey, and D. Szebesta, J. Opt. Soc. Am. B **11,** 886 (1994).
10. B. R. Judd, Phys. Rev. **127,** 750 (1962).
11. G. S. Ofelt, J. Chem. Phys. **37,** 511 (1962).
12. D. H. Huang, C. F. Li, and J. C. Zhong, Chin. J. Lasers (in Chinese) **25,** 1122 (1998).
13. M. J. Weber, J. Chem. Phys. **48,** 4774 (1968).
14. J. Wang, Y. H. Chen, and F. X. Gan, Acta Opt. Sin. (in Chinese) **16,** 78 (1996).
15. E. Sarantopoulou, Z. Kollia, A. C. Cefalas, V. V. Semashko, R. Y. Abdulsabirov, A. K. Naumov, S. L. Korableva, T. Szczurek, S. Kobe, and P. J. McGuiness, Opt. Commun. **208,** 345 (2002).
16. M. J. Weber, Phys. Rev. **157,** 262 (1967).
17. T. Kushida, J. Phys. Soc. Japan **34,** 1318 (1973).
18. T. Miyakawa, and D. L. Dexter, Phys. Rev. B **1,** 2961 (1970).
19. Y. Zhao, Opt. Commun. **134,** 470 (1997).